THE JOURNAL OF PHYSICAL CHEMISTRY C

Article

pubs.acs.org/JPCC

Graphene-Thickness-Dependent Graphene-Enhanced Raman Scattering

Xi Ling,[†] Juanxia Wu,[†,‡] Liming Xie,[§] and Jin Zhang*,[†]

[†]Center for Nanochemistry, Beijing National Laboratory for Molecular Sciences, Key Laboratory for the Physics and Chemistry of Nanodevices, State Key Laboratory for Structural Chemistry of Unstable and Stable Species, College of Chemistry and Molecular Engineering, Peking University, Beijing 100871, China

[‡]Academy for Advanced Interdisciplinary Studies, Peking University, Beijing 100871, China

[§]Key Laboratory of Standardization and Measurement for Nanotechnology of Chinese Academy of Sciences, National Center for Nanoscience and Technology, Beijing 100190, P. R. China

Supporting Information

ABSTRACT: Graphene-enhanced Raman scattering (GERS), enhancing Raman signals on graphene surface, is an excellent approach to investigate the properties of graphene via the Raman enhancement effect. In the present study, we studied the graphene-thickness dependent GERS in detail. First, by keeping molecule density on few-layer graphene using vacuum thermal deposition method, GERS enhancement was found to be the same for all graphene layers (one to six layers). While adsorbing probe molecules by solution soaking, the GERS enhancing factor was different on monolayer and bilayer graphene. By soaking in low concentration solutions, the GERS intensity on bilayer graphene was stronger than that on monolayer graphene, whereas by soaking under high concentration solutions, the GERS intensity difference was much less for that on monolayer and on bilayer. Molecule density, molecular configuration, and GERS enhancing factor are further discussed for molecules on monolayer and bilayer graphene. It was finally concluded that the abnormal graphene-thickness dependence of GERS between monolayer and bilayer graphene was attributed to the different enhancement for GERS on monolayer and bilayer graphene. Monolayer and bilayer graphene have different electronic structure and then doping effect of probe molecules, which shifts the Fermi level of graphenes differently. As a result, monolayer and bilayer graphene have different energy band matching with the probe molecules, yielding different chemical enhancement.

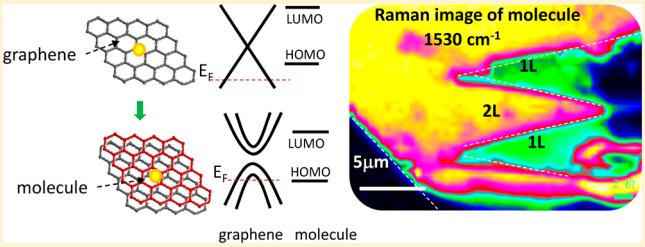

1. INTRODUCTION

Graphene-enhanced Raman scattering (GERS),[1] enhancing Raman signals of molecules on graphene, is a new phenomenon and has attracted intense interest recently. Much sensitive detection was achieved by combining GERS and noble-metal-based surface-enhanced Raman scattering (SERS).[2−4] Meanwhile, GERS paves a way for the studying of SERS on nonmetal materials.[5,6] Recently, not only graphene but also Si and Ge nanostructures were reported as Raman enhancement substrates,[6] which brings new understanding of the mechanism of Raman enhancement. In our previous work, to understand the mechanism of GERS, the dependence of GERS intensity on the distance of graphene and the probe molecule,[7] the molecular orientation,[8] the Fermi level position of graphene,[9] and the excitation wavelength[10] were investigated. It is now accepted that a chemical mechanism is the explanation for the GERS enhancement, yet more detailed Raman experiments are needed to further support the chemical mechanism.

The chemical mechanism strongly relies on the charge transfer between the energy bands of substrate and probe molecule. Because their energy band structures are different,[11] graphene with different layer numbers could have different GERS effects. A previous report found that both the monolayer graphene and few-layer graphene have a GERS effect, but a detailed layer-number-dependent GERS effect was not yet revealed.[1] After the discovery of GERS, Qiu[12] and Peimyoo[13] reported the monotonous decrease in GERS intensity as the layer number of graphene increases with the assumption of same molecule density adsorbed on *n*-layer graphene. Here we used vacuum thermal deposition to deposit probe molecules on a clean SiO_2/Si substrate and then transferred graphenes on that. In this way, the molecule density contacted with *n*-layer graphenes should be the same. The Raman measurement on the *n*-layer graphenes ($n < 6$) was carried out, and the graphene-thickness dependence of the GERS intensity is different from that of previous work.[12,13] Furthermore, because the solution soaking is an easy and widely used method in practical application, the GERS effect was investigated with the solution soaking method for molecule deposition. An abnormal graphene-thickness dependence of GERS intensity was found for molecules on monolayer and bilayer graphenes. This abnormal graphene thickness dependence of GERS was

Received: October 25, 2012
Revised: January 10, 2013
Published: January 14, 2013

dx.doi.org/10.1021/jp310564d | J. Phys. Chem. C 2013, 117, 2369−2376

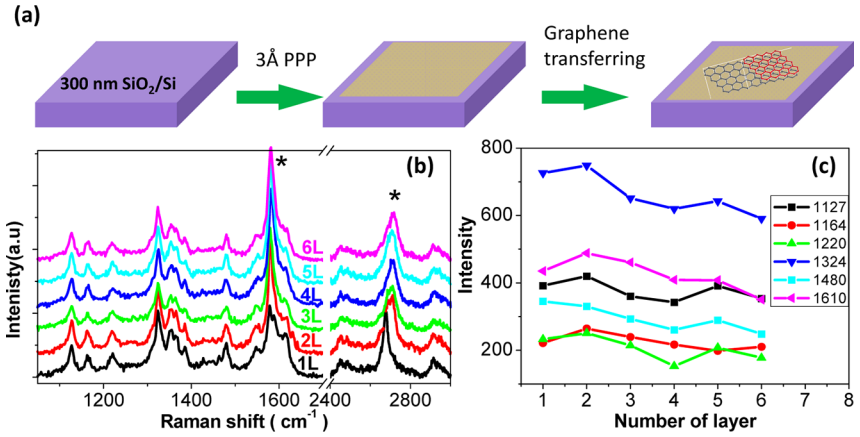

Figure 1. (a) Schematic illustration of the preparation of the sample. (b) Raman spectra comparison of equal PPP collected on different layers graphene. (c) Relative Raman intensity of the vibrational modes of PPP collected on different graphene layers. The different colors correspond to vibrational modes marked on the right side. The spectra were collected under the 514.5 nm laser excitation.

discussed in detail, and it was attributed to the doping-induced Fermi level shift of graphenes.

2. EXPERIMENTAL DETAILS

2.1. Chemical Materials. The probe molecules protopphyrin IX (PPP) purchased from Frontier Scientific, Inc. and copper(II) phthalocyanine (CuPc) and 4′-nitrobenzene-diazoaminoazobenzene (NAA) purchased from Alfa Aesar were used directly. PPP was deposited on the substrate by vacuum thermal deposition. CuPc was dissolved in a mixture of trifluoroacetic acid (TFAA) and dichloromethane (DCM) [1:10 (v/v)] to make a solution. The different concentrations of the CuPc solution were obtained by diluting gradually. NAA was dissolved in a trichloromethane solvent to make a solution.

2.2. Molecule Deposition. To investigate the thickness-dependent GERS effect accurately, it is critical to keep an equal number of the molecule on different graphene layers. However, it is difficult to satisfy the requirement of depositing molecules on the graphenes directly because the absorption process is selective to the surface. Here, as shown in Figure 1a, the probe molecule, such as protopphyrin IX (PPP) with a thickness of 3 Å, was deposited on a clean blank 300 nm SiO_2/Si substrate first by vacuum thermal deposition. Because the substrate is a uniform surface, the number of molecules on every area can be thought to be the same. After that, graphene was transferred on the top of the molecule layer by mechanical exfoliation. Thus, the number of molecules in contact with the different graphene layers should be the same. The optical image, AFM (atomic force microscopy) and Raman spectra were used to determine the layer number of the graphenes (see part 1 in the Supporting Information).

2.3. Raman Measurement. The Raman spectra were collected using a Horiba-Jobin Yvon Labram HR800 instrument with a 632.8 nm He−Ne laser and a 514.5 nm Ar+ laser. An XYZ stage with micrometer accuracy was used to move the sample during the Raman mapping experiment. A 100× objective was used to focus the laser beam. The laser power was controlled below 1 mW to avoid the decomposition of molecules and the heating effect. The spectra in comparison were obtained under the same condition. The spectrum parameters of the peaks were obtained after fitting them with Lorentzian function. To avoid the heterogeneity from the substrate, we focused the Raman spectra measurement on the graphenes including different layers in the same area.

3. RESULTS AND DISCUSSION

3.1. Investigation of the Graphene-Thickness-Dependent GERS Effect. Figure 1b shows Raman spectra of PPP molecules on one- to six-layer graphenes, where Raman frequency and GERS intensity for PPP on different graphene layers are almost the same. Figure 1c plots the intensity of different vibrational modes of PPP (1127, 1164, 1220, 1324, 1480, 1610 cm^{-1}) against the number of graphene layers. From one to six layers, the intensity change is within 20%. Taking the vibrational mode 1324 cm^{-1} as example, on monolayer graphene, the intensity is about 700 counts, whereas on the six-layer graphene, it is about 600 counts. Considering that the absorption is ∼2.3% for one-layer graphene,[14] it should be 13.8% for six-layer graphene. Then, the GERS intensity on six-layer graphene should be 99 counts (700/(1 − 2.3%) × 13.8% = 99) weaker than that on the monolayer graphene, which is consistent with the experimental data (700 − 600 = 100). Hence, the imperceptible Raman intensity difference among the one- to six-layer graphenes is induced by the loss of the light when propagating in the graphene layers, which induces the contribution of the interference enhancement from the SiO_2/Si substrates to be different.[15] Thus, we come to a conclusion that the GERS intensity induced by the chemical effect on one- to six-layer graphenes is less different. The similar result is obtained for CuPc molecules (see part 2 in the Supporting Information).

Compared with the previous works in which GERS intensity decreased as graphene layer number increased,[12,13] this work draws a different conclusion. This could be due to the invalid assumption of equal molecule density on the different graphene layers in the previous work.[12,13] This work gives a more accurate result because the thermal deposition method used here should give an identical molecule density on different graphene layers, whereas solution soaking used in these reports should give different molecule density on different graphene layers because different graphene layers have different surface properties (like potential, morphology, and so on) .

3.2. Abnormal Graphene Thickness Dependence in GERS. Because the chemical mechanism is mainly dependent on the relative position of the energy bands of the probe

dx.doi.org/10.1021/jp310564d | J. Phys. Chem. C 2013, 117, 2369−2376

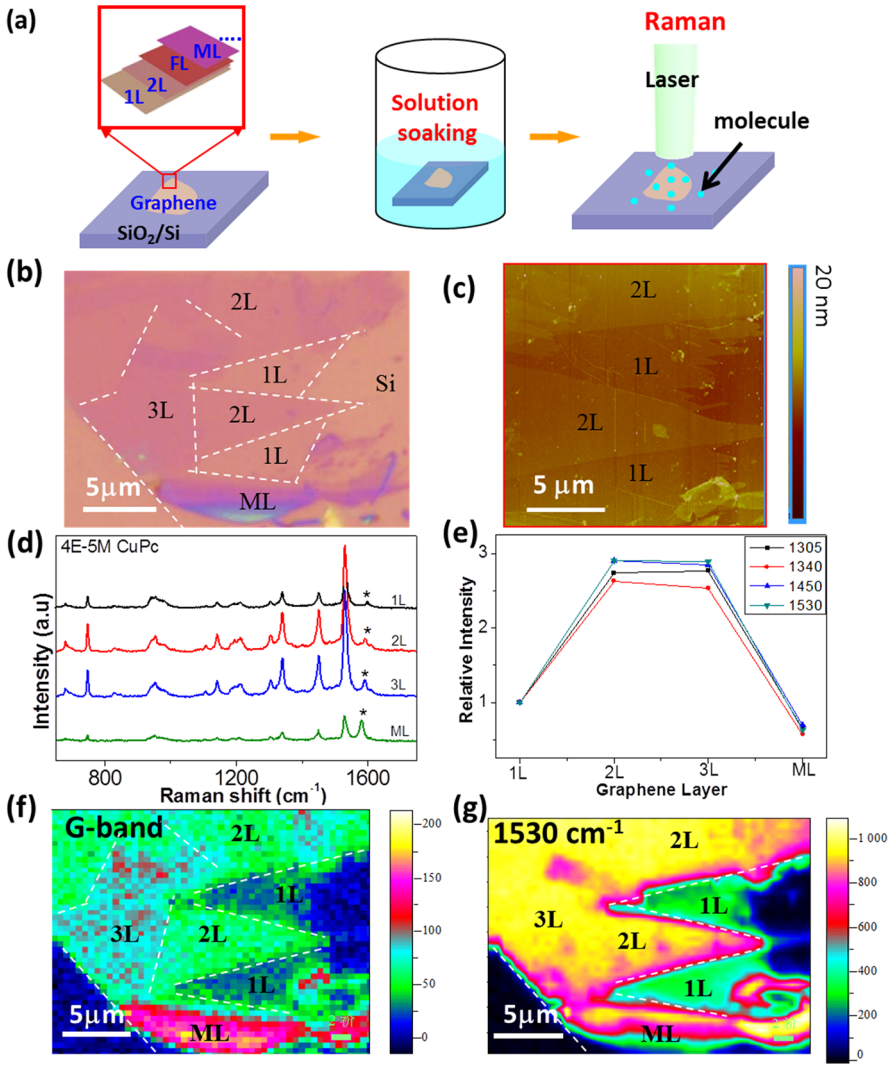

Figure 2. (a) Schematic illustration of the experimental processes. (b) Optical image of graphenes including mono-, bi-, tri-, and multilayer graphene. (c) Corresponding AFM image. (d) Raman spectra of CuPc deposited on mono-, bi-, tri-, and multilayer graphene under 4×10^{-5} mol/L concentrations. (e) Relative intensity of the Raman signals of CuPc on different layer graphenes. The intensities were normalized by the signals on monolayer graphene. The different color lines stand for the peaks marked on the up right corner. (f–g) Raman mapping images of the G band from graphenes (f) and the 1530 cm^{-1} peak from CuPc (g) corresponding to (b) after 4×10^{-5} mol/L CuPc soaking. All of the spectra were collected under the 632.8 nm laser excitation.

molecule and the substrate, the GERS effect for monolayer and bilayer graphene should be similar in regards to the fact that the Fermi levels of the pristine monolayer and few-layer are at the Dirac point. However, the GERS intensity is observed higher on monolayer than that on bilayer graphene when depositing the molecule by solution soaking. Taking CuPc molecule as probe molecule and a mixture of TFAA and DCM [$CF_3COOH \bullet CH_2Cl_2$, 1:10 (v/v)] as solution, the solution soaking method was used to deposit the CuPc molecule on graphene layers, as shown in Figure 2a. It should be noted that the CuPc molecule will induce n-doping to graphene, whereas CF_3COOH will induce p-doping to graphene. Thus, the doping degree can be different by changing the concentration of CuPc molecule. Usually, graphenes were soaked in the molecule solution for ~30 min to reach the adsorption–desorption equilibrium and then rinsed in the pure solvent for several mins to remove the free molecules. Figure 2b–g shows typical Raman spectra of CuPc on graphene by soaking the graphenes in a 4×10^{-5} mol/L CuPc solution. Figure 2b is the optical image of the graphenes. The areas of the different layers graphene were marked using the dashed lines. Because of the low CuPc concentration, the adsorption is submonolayer. AFM imaging of the soaked sample (Figure 2c) shows clean surfaces as pristine graphenes, and the adsorbed CuPc molecules could not be resolved. Figure 2d shows that the Raman signals of CuPc on the monolayer graphene are weaker than those on the bilayer and trilayer graphenes. Figure 2e plots the relative intensity of CuPc Raman signals on different layers graphenes. Roughly, the Raman signals are decreased as the number of graphene layers increased.[1] Opposite from the reference result where the GERS intensity of the molecule is the largest on monolayer graphene,[12] here we find that the Raman intensity of CuPc on bilayer is stronger than that on monolayer. The Raman images of the G band from graphene and the Raman peak 1530 cm^{-1} from CuPc are shown in Figure 2f,g, respectively. The image in Figure 2f shows that the G-band intensity is increasing with the increase in the graphene layers, which is consistent with refs 16 and 17. The distribution of the

dx.doi.org/10.1021/jp310564d | J. Phys. Chem. C 2013, 117, 2369–2376

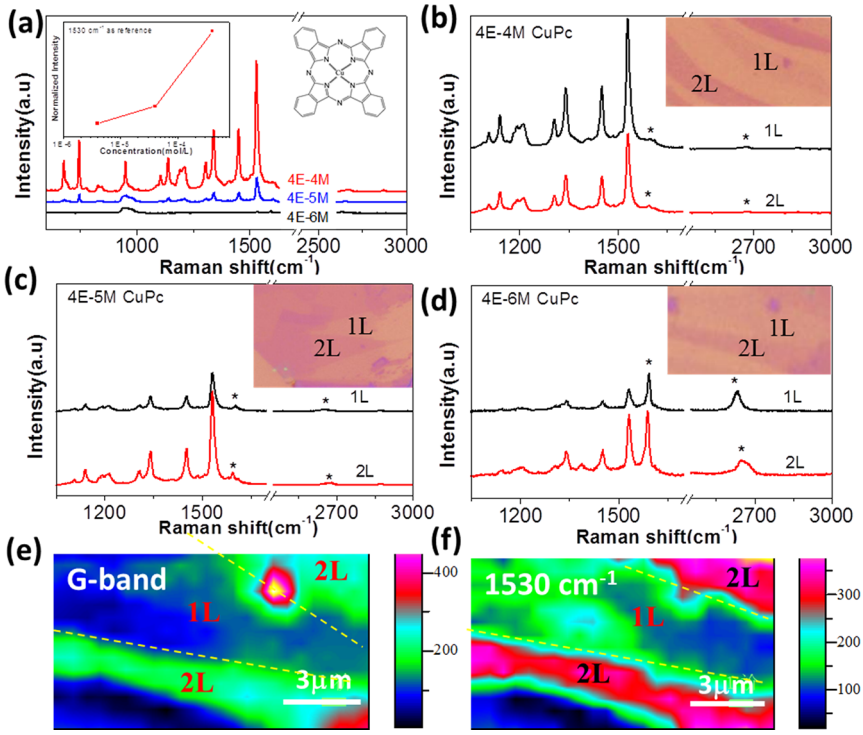

Figure 3. (a) Raman spectra of CuPc deposited on monolayer graphene by solution soaking under different concentrations. The inset is the curve of the relative Raman intensity of 1530 cm^{-1} peak of CuPc as a function of the concentration. (b–d) Comparison of the Raman spectra of CuPc deposited on monolayer and bilayer graphene under different concentrations. (b) 4×10^{-4} mol/L, (c) 4×10^{-5} mol/L, and (d) 4×10^{-6} mol/L. The inset is the corresponding optical images. (e–f) Eaman mapping images of the G band from graphenes (e) and the 1530 cm^{-1} peak from CuPc (f), corresponding to the graphenes in panel d. All of the spectra were collected under the 632.8 nm laser excitation.

Raman intensity of CuPc molecule in Figure 2g indicates that the molecules were homogeneously adsorbed on graphene layers. However, on different layers of graphene, the CuPc Raman intensity differs. The obvious boundary between the monolayer and the bilayer graphenes shows the stronger GERS intensity on bilayer graphene than that on monolayer graphene, whereas the difference between the bilayer and trilayer graphene is not so large because the boundary is ambiguous.

3.3. Possible Explanation for the Abnormal Phenomenon. To investigate the reason of the abnormal thickness dependence of the GESR intensity on monolayer and bilayer graphenes, we should consider several factors: (1) the molecule density variation; (2) the different molecular configuration; and (3) the different GERS enhancing. First, to consider whether it is due to the molecule density variation, the thickness-dependent GERS effect was investigated by using different probe molecule concentrations. As shown in Figure 3a, when graphene was soaked with the increasing concentrations (4×10^{-4}, 4×10^{-5}, 4×10^{-6} mol/L) of the CuPc solution, the obtained GERS intensity increased, which implies the increased number of the adsorbed molecules. In the inset of Figure 3a, it shows the curve of the Raman intensity as a function of the concentration. For the adsorption under low concentration, it will follow the Langmuir isotherm. Before it gets to the maximum amount adsorbed, the coverage is almost increasing linearly with the increase in the concentration, and it will become saturated after all of the adsorption sites were occupied. Therefore, if the adsorption is high to monolayer, then the Langmuir isotherm will get saturated with the further increase in the concentration. Because the three used concentrations are all in the unsaturated range of the Langmuir isotherm, the adsorption under these concentrations was submonolayer. Figure 3b–d shows the Raman spectra collected on monolayer and bilayer after adsorbing CuPc molecules by solution soaking with different concentrations. For high concentrations, such as 4×10^{-4} mol/L, the GERS intensity on the monolayer graphene is less different from that on bilayer graphene, as shown in Figure 3b, which is consistent with the result in Figure 1. However, when the concentration decreases to 4×10^{-5} and 4×10^{-6} mol/L, as shown in Figure 3c,d, the bilayer graphene shows a higher GERS intensity. The Raman images of the G band from graphene and the peak 1530 cm^{-1} from the CuPc molecules in Figure 3e,f are similar to that in Figure 2f,g, but correspond to the concentration 4×10^{-6} mol/L. Hence, we can conclude that the abnormal phenomenon is strongly related to the concentration. The result in Figure 3 indicates the abnormal phenomenon is not due to the different molecule densities, or else, under the concentration of 4×10^{-4} mol/L, the GERS intensity on bilayer graphene should be stronger than that on monolayer, as that under the concentration 4×10^{-5} and 4×10^{-6} mol/L, but the fact is it is not.

Another factor that should be considered is the difference of the molecular configuration. As reported in our previous work,[8] molecular configuration can influence the GERS intensity. As we know, in chemical mechanism, the difference of the molecular configuration will influence not only the absolute intensity but also the relative intensity of the signals. Hence, by comparing the GERS intensity and Raman frequency of CuPc molecules on monolayer and bilayer graphene, we can infer whether the molecular configuration is the same or not. As shown in Table 1, it is clear to see that the GERS intensity is two times stronger on the bilayer graphene than that on the monolayer graphene for all of the vibrational modes. Also, the

dx.doi.org/10.1021/jp310564d | J. Phys. Chem. C 2013, 117, 2369–2376

Table 1. Comparison of the Raman Intensity and Raman Shift of the CuPc Molecules Deposited on Monolayer and Bilayer Graphene by Solution Soaking under a 4×10^{-5} mol/L Solution

Raman mode (cm^{-1})	I_{2L}/I_{1L}	$\Delta\omega$ (cm^{-1})
679.2	2.2	0.2
685.7	1.7	0.9
746.9	1.9	−0.2
1106.4	2.3	−0.4
1140.3	2.1	−0.07
1189.45	1.7	0.3
1211.7	2.2	−0.1
1305.9	2.2	−0.01
1340.8	2.2	−0.09
1451.7	2.5	0.1
1532.9	2.5	−0.6

Raman shift for the vibrational modes is almost no change on bilayer and monolayer graphene. Both of them indicate that the molecular configuration is the same on bilayer and monolayer graphene. Thus, the difference of the molecular configuration was excluded as the reason for the abnormal phenomenon.

As reported, graphene can be doped by organic molecules.[18−20] A direct evidence to prove the doping effect is the Raman shift.[21,22] For graphene, p-doping can upshift the G and G′ bands and vice versa.[22] Figure 4 shows the Raman spectra of

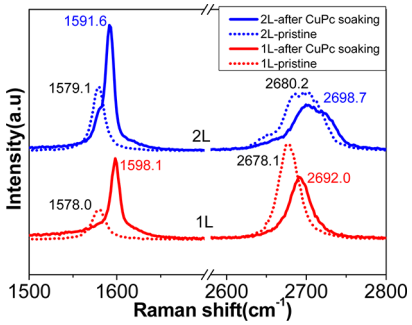

Figure 4. Variation of the G and G′ bands of monolayer (red line) and bilayer (blue line) graphene before (dashed lines) and after (solid lines) soaking in 4×10^{-5} mol/L CuPc solution. The spectra were collected under the 514.5 nm laser excitation to avoid the disturbance from the Raman signals of the molecules.

monolayer (red lines) and bilayer (blue lines) graphene before (dashed lines) and after (solid lines) CuPc solution soaking. To avoid the disturbance from the Raman signals of the molecules, the spectra were excited under 514.5 nm laser line, where the Raman signals from the molecules were very weak. Raman fitting results are listed in Table 2. The upshift of the G and G′ bands as well as the decrease in the $I_{G'}$ and I_G ratio indicates that graphene was p-doped. However, as mentioned before, in the solution, CuPc molecule will contribute n-doping to graphene, whereas the CF_3COOH molecule will contribute p-doping to graphene. They are competitive to the doping of graphene. Thus, the result indicates that the CF_3COOH molecule works dominantly because it is a majority under such low concentration. Meanwhile, the full width at half-maximum (FWHM) become narrower after molecules deposition. It contributed to the blockage of the decay channel of phonons into electron−hole pairs due to the Pauli exclusion and consequently the increasing lifetime.[13] Besides, the split of the G band of bilayer graphene is the result of the Kohn anomaly induced by the doping.[16,23] The doping on graphene will induce two main effects on the electron energy band structure of graphene. The one is the shift of the Fermi level. For p-doping, the Fermi level will shift to lower energy, whereas for n-doping, it will shift to higher energy. The shift of the G band is dependent on the shift of the Fermi level and can be expressed as:[24]

$$\hbar\omega_G - \hbar\omega_G^0 = \lambda\left\{|E_F| + \frac{\hbar\omega_G}{4}\ln\left|\frac{2|E_F| - \hbar\omega_G}{2|E_F| + \hbar\omega_G}\right|\right\}$$

$$E_f = -\frac{\gamma_1}{2} + \frac{1}{2}\sqrt{\frac{4\pi\gamma^2 C_G}{e}|V_g - V| + \gamma_1} \quad (1)$$

where ω_G^0 is the frequency of the G band (ω_G) at the Dirac point, $\lambda = A_{uc}D^2/2\pi\hbar\omega_G M v_F^2$, $|E_F|$ is the absolute value of the Fermi energy with respect to the Dirac point, A_{uc} is the area of the graphene unit cell, M is the carbon atom mass, and D is the electron−phonon coupling strength. The other one is the opening of the energy gap. For pristine monolayer and bilayer graphenes, there is no gap between the conduction band and valence band, whereas it is tunable by the electric field or doping. It was reported that a band gap up to 0.25 eV can be achieved for bilayer graphene by a variable external electric field.[25] In our previous work,[9] by adding an tunable electric field, the Fermi level of graphene was modified, and it was found that the GERS intensity can be modulated. It should be noted that the abnormal graphene-thickness dependence of GERS is not only observed for CuPc molecules. Some more kinds of molecules are carried out, such as NAA, shown in part 3 of the Supporting Information.

Figure 5 shows the variation of the Raman spectroscopy of one- to three-layer graphene with the solution concentration. Figure 5a−c is excited by the 514.5 nm laser line, where the CuPc Raman spectra is out of the resonant condition and then very weak, whereas Figure 5d−f is excited by the 632.8 nm laser, where the Raman signals at around 1450 and 1530 cm^{-1} are from the CuPc molecules. For either 514.5 or 632.8 nm excitation, the shift of the G and G′ bands shows a similar trend for CuPc on monolayer, bilayer, or trilayer graphene. Shown in Figure 5g is the Raman shift of the G band excited by the 632.8 nm laser as a function of the soaking concentration. At the low

Table 2. Variation of the Raman Spectrum Parameters of the Monolayer and Bilayer Graphene before and after CuPc Solution Soaking[a]

	G-band shift (cm^{-1})		G′-band shift (cm^{-1})		G (FWHM)		$I_{G'}/I_G$	
layer number	pristine	after CuPc soaking	pristine	after CuPc soaking	pristine	after CuPc soaking	pristine	after CuPc soaking
1L	1578.0	1589.1	2678.1	2689.0	19.4	13.7	3.28	0.78
2L	1579.1	1591.6	2680.2	2698.7	16.1	12.2		

[a]Data are from the spectra in Figure 4.

dx.doi.org/10.1021/jp310564d | J. Phys. Chem. C 2013, 117, 2369−2376

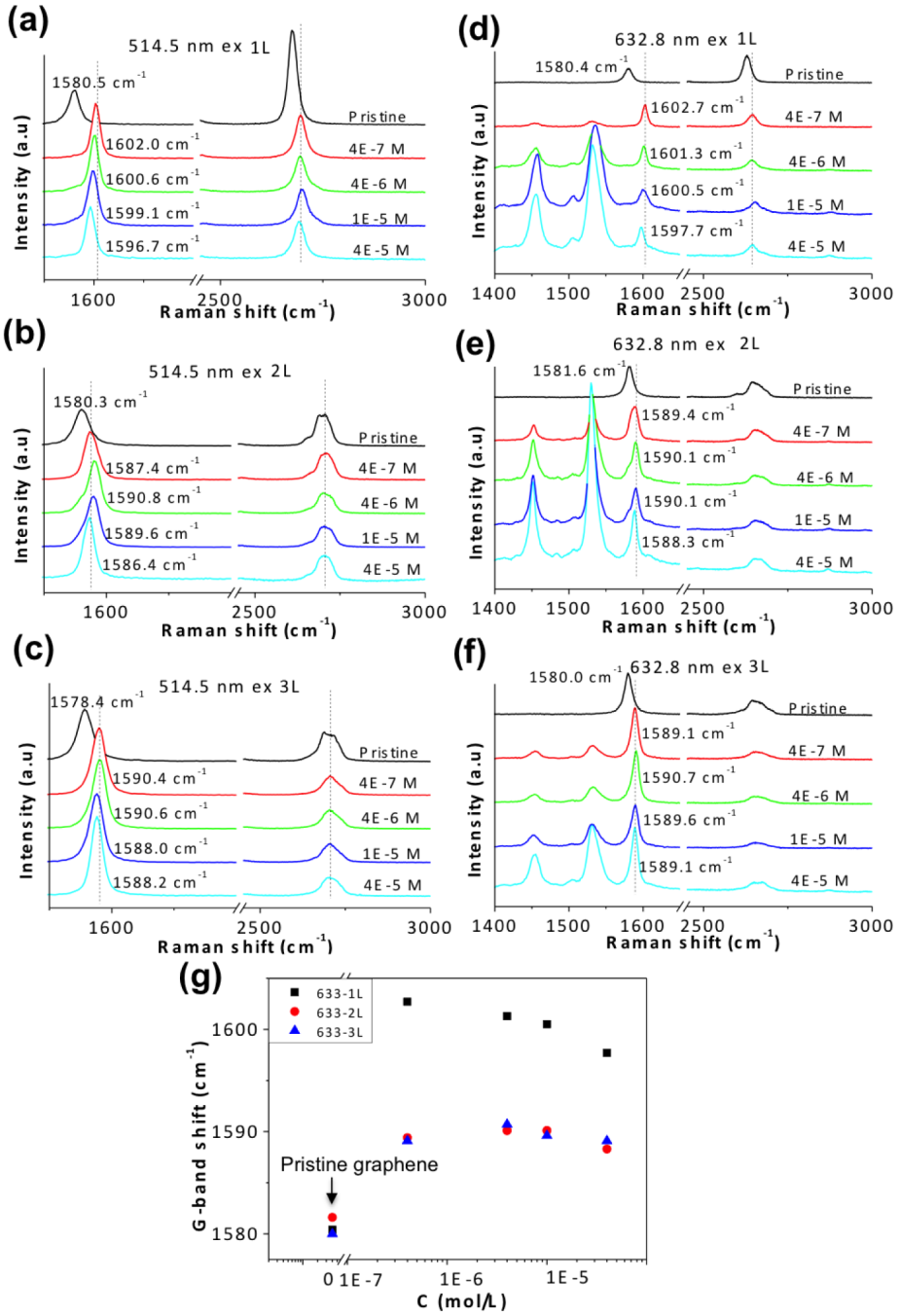

Figure 5. Raman spectra of mono- (a,d), bi- (b,e), and trilayer (c,f) graphene after soaking in the CuPc molecules solution from low to high concentration (4×10^{-7}, 4×10^{-6}, 1×10^{-5}, 4×10^{-5} mol/L). (a–c) Excited by the 514.5 nm laser and (d–f) excited by the 632.8 nm laser. Except the G and G′ bands, the other Raman signals in panels d–f are from the CuPc molecules. (g) Variation of the G-band shift of graphene with the soaking concentration, where the data are from panels d–f.

concentration, the upshift of the G band is the largest, whereas with the concentration increasing, the G band tends to red-shift gradually back to the pristine position. Besides, the change of the Raman shift on the monolayer graphene is larger than that on the bilayer and trilayer graphene, which indicates that the monolayer graphene is more sensitive to doping. As shown in eq 1, the corresponding shift of the Fermi level can be calculated from the G-band shift. The result is shown in Table 3. On monolayer graphene, the Fermi level shifts down to about −0.4 eV when soaking at low concentration solution (4×10^{-7} mol/L), whereas on bilayer and trilayer graphene, it is about 0.15 and 0.2 eV, respectively. (Here, for bilayer and trilayer graphene, we ignore the different electron–phonon coupling strength due to interlayer interaction to the change of the Fermi level and use the same equation to get the position of the Fermi level.) When the concentration increases to 4×10^{-5} mol/L, the Fermi level changes to 0.35 eV for monolayer and 0.17 eV for bilayer and trilayer. Thus, we can conclude the relationship of the energy band of graphene and the CuPc molecule in Figure 6. We assume that the change of the energy level of CuPc molecule under different concentrations can be neglected. Then, the change of the Fermi level of graphene can

dx.doi.org/10.1021/jp310564d | J. Phys. Chem. C 2013, 117, 2369–2376

Table 3. Raman Shift of the G Band of One to Three Layers Graphene after Soaking under Different Concentrations and the Corresponding Fermi Level Position[a]

	514-1L		514-2L		514-3L	
C (mol/L)	ω_G (cm^{-1})	$\lvert E_F \rvert$ (eV)	ω_G (cm^{-1})	$\lvert E_F \rvert$ (eV)	ω_G (cm^{-1})	$\lvert E_F \rvert$ (eV)
0.00	1580.5	0	1580.3	0	1578.4	0
4.00×10^{-7}	1602	0.4	1587.4	0.15	1590.4	0.2
4.00×10^{-6}	1600.6	0.38	1590.8	0.2	1590.6	0.2
1.00×10^{-5}	1599.1	0.37	1589.6	0.2	1588	0.17
4.00×10^{-5}	1596.7	0.35	1586.4	0.16	1588.2	0.17

[a]Data are from the spectra in Figure 5a−c.

influence the matching of energy band of graphene and the CuPc molecule. As shown in Figure 6, at the low concentration, the Fermi level of monolayer graphene is much lower than the HOMO of the CuPc molecule, and it is higher for bilayer graphene. Meanwhile, the electron density, which will influence the GERS effect by the electron−phonon coupling, is larger on bilayer graphene than that on monolayer graphene.[26] Both of the two reasons induced the stronger GERS intensity on bilayer than that on monolayer at low concentration. However, at high concentration, the Fermi level of both the monolayer and the bilayer will shift back to the Dirac point, and the difference between them will be smaller and smaller. Thus, the GERS intensity on monolayer and bilayer graphene is less different. This is the reason for the abnormal thickness dependence of GERS intensity on monolayer and bilayer graphene.

4. CONCLUSIONS

In conclusion, detailed thickness-dependent GERS intensity was investigated by controlling molecule density. It shows the GERS effect is independent of the number of graphene layers in the six layers range. Furthermore, we discussed the abnormal thickness dependence on monolayer and bilayer graphene when adsorbing CuPc molecules by solution soaking. It was found when soaking at low concentrations that the GERS intensity on bilayer graphene is much stronger than that on the monolayer graphene, whereas they are almost the same at high concentrations. The reason was analyzed by considering the influence from the molecule density, the molecular configuration, and the degree of GERS effect. It was finally concluded to be the contribution from the doping-induced shift of the Fermi level of graphene and consequently the change of the match degree of the energy band of graphene and the molecule, which will influence the strength of the chemical enhancement.

■ ASSOCIATED CONTENT

Supporting Information

Determination of the layer numbers of graphenes, investigation of graphene thickness dependence of the GERS intensity by taking the CuPc molecule as Raman probe, and GERS spectra of NAA on monolayer and bilayer graphene by solution soaking. This material is available free of charge via the Internet at http://pubs.acs.org.

■ AUTHOR INFORMATION

Corresponding Author

*Tel/Fax: 86-10-6275-7157. E-mail: jinzhang@pku.edu.cn.

Notes

The authors declare no competing financial interest.

■ ACKNOWLEDGMENTS

This work was supported by NSFC (21233001, 21129001, and 51121091), MOST (2011CB932601) and Beijing Municipal Natural Science Foundation (No. 2132056).

■ REFERENCES

(1) Ling, X.; Xie, L. M.; Fang, Y.; Xu, H.; Zhang, H. L.; Kong, J.; Dresselhaus, M. S.; Zhang, J.; Liu, Z. F. *Nano Lett.* **2010**, *10* (2), 553−561.

(2) He, S. J.; Liu, K. K.; Su, S.; Yan, J.; Mao, X. H.; Wang, D. F.; He, Y.; Li, L. J.; Song, S. P.; Fan, C. H. *Anal. Chem.* **2012**, *84* (10), 4622−4627.

(3) Xu, W. G.; Ling, X.; Xiao, J. Q.; Dresselhaus, M. S.; Kong, J.; Xu, H. X.; Liu, Z. F.; Zhang, J. *Proc. Natl. Acad. Sci. U.S.A.* **2012**, *109* (24), 9281−9286.

(4) Zhao, H.; Fu, H. G.; Zhao, T. S.; Wang, L.; Tan, T. X. *J. Colloid Interface Sci.* **2012**, *375*, 30−4.

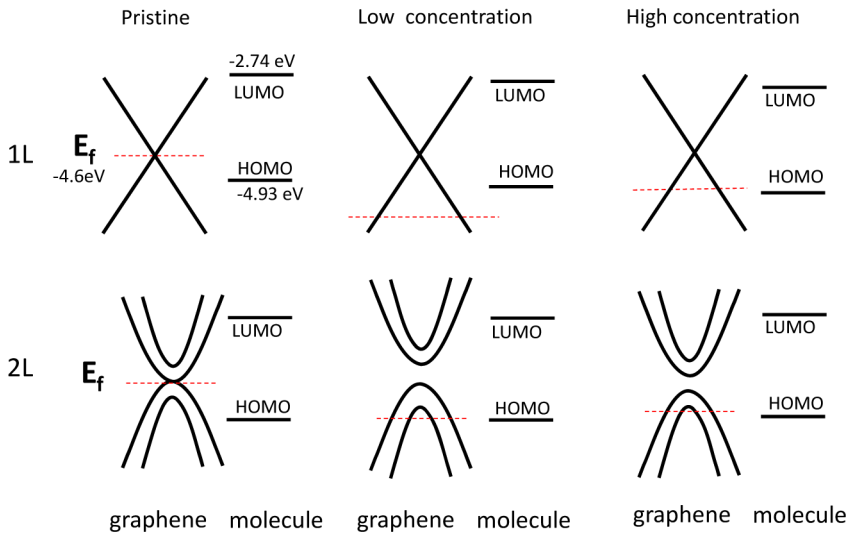

Figure 6. Schematic illustration of the variation of the energy band structure of monolayer and bilayer graphene after molecules doping under low and high concentrations soaking.

dx.doi.org/10.1021/jp310564d | *J. Phys. Chem. C* 2013, 117, 2369−2376

(5) Kong, X. K.; Chen, Q. W.; Li, R.; Cheng, K.; Yan, N.; Chen, J.; Zhou, Y. M. *Chem. Phys. Chem.* **2012**, *13* (6), 1449−1453.
(6) Wang, X. T.; Shi, W. S.; She, G. W.; Mu, L. X. *J. Am. Chem. Soc.* **2011**, *133* (41), 16518−16523.
(7) Ling, X.; Zhang, J. *Small* **2010**, *6* (18), 2020−2025.
(8) Ling, X.; Wu, J. X.; Xu, W. G.; Zhang, J. *Small* **2012**, *8* (9), 1365−1372.
(9) Xu, H.; Xie, L. M.; Zhang, H. L.; Zhang, J. *Acs Nano* **2011**, *5* (7), 5338−5344.
(10) Ling, X.; Moura, L. G.; Pimenta, M. A.; Zhang, J. *J. Phys. Chem. C* **2012**, *116* (47), 25112−25118.
(11) Gruneis, A.; Attaccalite, C.; Wirtz, L.; Shiozawa, H.; Saito, R.; Pichler, T.; Rubio, A. *Phys. Rev. B* **2008**, *78* (20), 205425-1−205425-16.
(12) Qiu, C. Y.; Zhou, H. Q.; Yang, H. C.; Chen, M. J.; Guo, Y. J.; Sun, L. F. *J. Phys. Chem. C* **2011**, *115* (20), 10019−10025.
(13) Peimyoo, N.; Yu, T.; Shang, J. Z.; Cong, C. X.; Yang, H. P. *Carbon* **2012**, *50* (1), 201−208.
(14) Skulason, H. S.; Gaskell, P. E.; Szkopek, T. *Nanotechnology* **2010**, *21* (29), 295709-1−295709-8.
(15) Ling, X.; Zhang, J. *J. Phys. Chem. C* **2011**, *115* (6), 2835−2840.
(16) Malard, L. M.; Pimenta, M. A.; Dresselhaus, G.; Dresselhaus, M. S. *Phys. Rep.* **2009**, *473* (5−6), 51−87.
(17) Wang, Y. Y.; Ni, Z. H.; Shen, Z. X.; Wang, H. M.; Wu, Y. H. *Appl. Phys. Lett.* **2008**, *92* (4), 043121-1−043121-3.
(18) Pinto, H.; Jones, R.; Goss, J. P.; Briddon, P. R. *J. Phys.: Condens. Matter* **2009**, *21* (40), 402001-1−402001-3.
(19) Voggu, R.; Das, B.; Rout, C. S.; Rao, C. N. R. *J. Phys.: Condens. Matter* **2008**, *20* (47), 472204-1−472204-5.
(20) Wang, X. M.; Xu, J. B.; Xie, W. G.; Du, J. *J. Phys. Chem. C* **2011**, *115* (15), 7596−7602.
(21) Dong, X. C.; Shi, Y. M.; Chen, P.; Ling, Q. D.; Huang, W. *Jpn. J. Appl. Phys.* **2010**, *49* (1), 01AH4.
(22) Ferrari, A. C. *Solid State Commun.* **2007**, *143* (1−2), 47−57.
(23) Wang, K. A.; Rao, A. M.; Eklund, P. C.; Dresselhaus, M. S.; Dresselhaus, G. *Phys. Rev. B* **1993**, *48* (15), 11375−11380.
(24) Yan, J.; Zhang, Y. B.; Philip, K.; Pinczuk, A. *Phys. Rev. Lett.* **2007**, *98*, 166802-1−166802-4.
(25) Ohta, T.; Bostwick, A.; Seyller, T.; Horn, K.; Rotenberg, E. *Science* **2006**, *313* (5789), 951−954.
(26) Castro Neto, A. H.; Guinea, F.; Peres, N. M. R.; Novoselov, K. S.; Geim, A. K. *Rev. Mod. Phys.* **2009**, *81* (1), 109−162.